Solar collector exergetic optimization for a multi effect humidification desalination prototype

Raúl González-Acuña[1], Freddy Malpica[2] and Pedro Pieretti[3]
[1]Instituto de Energía - Universidad Simón Bolívar, Universidad Simón Bolívar, 1080, Caracas, Venezuela, regonzalez@usb.ve
[2]Departamento Termodinámica y Fenómenos de Transferencia, Universidad Simón Bolívar, 1080, Caracas, Venezuela, fmalpica@usb.ve
[3]Instituto de Energía - Universidad Simón Bolívar, ppieret@usb.ve

ABSTRACT

Venezuela is a country with a great deal of water resources. In spite of this, about 1.6 million inhabitants are dispersed in remote regions where water distribution is problematic due to the lack of this resource. A flat plate solar collector was built as a component of a single-stage Multi-Effect Humidification (MEH) desalination plant prototype, and its characterization was done on a testing rig designed and constructed according to the ANSI/ASHRAE 93-2003 standards. In order to optimize the operation of this equipment, the exergetic change of the working fluid across the solar collector was maximized. This objective was accomplished through a numerical simulation of the solar collector performance using a predictive algorithm and available yearlong meteorological data. It was found that a mass flow rate equal to 0.006 kg/s (0.36 LPM) should be maintain to ensure the maximum exergetic gain of the working fluid for an inlet temperature of 54°C.

Keywords: Desalination, Solar Collector, Optimization, Humidification, Standard

NOMENCLATURE

A	cross-sectional area (m^2)
C_p	specific heat capacity (J/kg K)
F'	efficiency factor (dimensionless)
F''	flow factor (dimensionless)
F_R	heat removal factor (dimensionless)
I	solar irradiance (W/m^2)
$K_{\tau a}$	Incidence angle modifier (dimensionless)
$\dot{m}$	mass flow (kg/s)
$\dot{q}$	heat flow (W)
RH	relative humidity (%)
S	absorber input heat flow per unit of area (W/m^2)
T	temperature (K)
U	global heat transfer coefficient (W/m^2 K)/Internal Energy (J)
V	volume (m^3)
W	reversible work (J)

GREEK

α	absorptivity (dimensionless)
ΔT	temperature difference (K)
η	efficiency (dimensionless)
τ	transmissivity (dimensionless)
($\tau\alpha$)	transmissivity-absorptivity product

SUBSCRIPT

1	state 1
2	state 2
a	aperture
amb	ambient
c	collector
e	effective
en	energy
ex	exergy
fi	fluid inlet
fm	mean fluid
fo	fluid outlet
in	Input
L	loss
l	without edges
n	normal
o	including fluid thermal resistance
p	Petela
pm	mean plate
sun	Sun
u	useful

1. INTRODUCTION

The problem of water shortage is affecting population all around the world. According to the FAO, 1800 million people will live in countries, such as China and Pakistan, where water needs will become critical in 2025 [1]. To face this situation, researches and studies have been made in order to find an alternative way to obtain water for human consume, at this point the conventional desalination plants show up as a feasible option; nevertheless, these facilities contribute to the emission of greenhouse gases. A proposal way to stop this trend is to use renewable sources, especially in coastal areas where solar irradiation and wind speed are abundant.

Venezuela is a country with a great deal of water resources, as a consequence of its location in the Amazon Basin. In spite of this, about 1.6 million inhabitants are dispersed in remote regions such as *Península de Paraguaná* (*Falcón* State), where water distribution is problematic due to the lack of this resource, but at the same time solar irradiance and wind speed are very high and relatively constant throughout the year at this location. The Institute of Energy of the Simon Bolivar University established a desalination research branch, in order to face the insufficient water availability in remote locations, starting with the fishermen communities that work near Dos Mosquises cay in Los Roques National Park, a set of cays located in the Caribbean Sea at 86 miles from Vargas State's coast.

The project focused on the development of a 25 liters per day single-stage Multi-Effect

Humidification (MEH) desalination plant using a flat plate solar collector. The prototype was designed considering the following criteria: low initial and maintenance costs, easy transportation, low energy consumption, and the utilization of as many homemade components as possible.

A single-stage MEH unit, as shown in Figure 1, consists of three main processes: evaporation, dehumidification and solar heating. The first two occur in the humidifier and dehumidifier, respectively. In the humidifier, water vapor is transferred to an air stream; later, in the dehumidifier, the air stream is cooled to obtain distillated water. Brine is collected from the bottom of the humidifier. Solar heating takes place in the solar collector, where seawater receives its main energy input.

In order to face irradiance variability, González *et al.* [1] proposed the installation of a by-pass valve (see Figure 1) to control the solar collector discharge temperature by means of regulating the mass flow rate. It has been shown by Luminosu and Fara [2] that solar collector outlet temperature depends simultaneously, without maximum points, both on the mass flow rate and collecting area, which gives as a result, that the only way to determine the optimal operation procedure of this equipment is by an exergetic analysis.

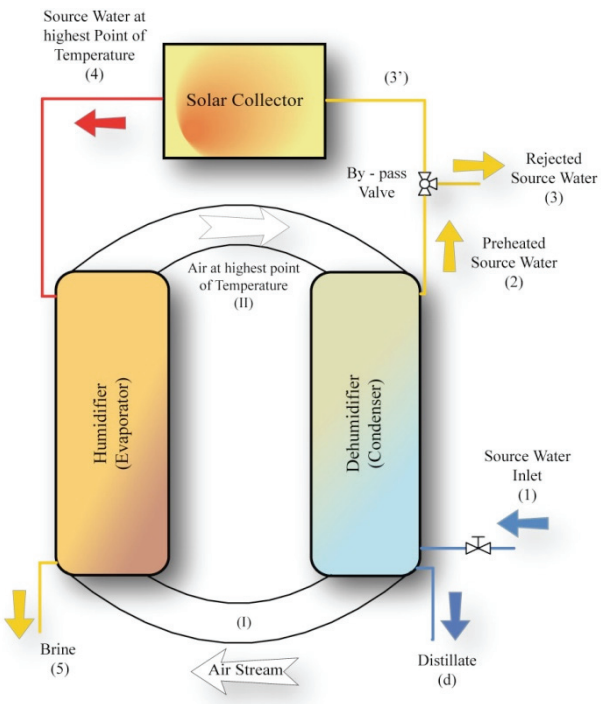

Figure 1. Schematic of a MEH desalination unit [1]

The aim of this paper is to establish the mass flow required to maximize the exergy change of the working fluid across a sandwich type flat plate solar collector during a normal operation of the desalination plant. This was done by a numerical simulation using a

predictive algorithm and an available yearlong meteorological data. The prediction algorithm was validated against experimental data obtained from the characterization tests based on the ANSI/ASHRAE 93-2003 standard [3] requirements.

2. FLAT PLATE SOLAR COLLECTOR

Constructive components normally found in a flat plate solar collector are shown in Figure 2, and they are: transparent cover, absorbing plate, thermal insulation and casing.

The transparent cover produces the greenhouse effect and reduces convection losses to the environment, improving the equipment performance. Depending on the process temperature, weather condition or irradiance, solar collectors must have a double cover. This favors the greenhouse effect and, therefore, increases the temperature which may be reached by the working fluid. However, radiative properties of the cover are affected by this arrangement, so less energy enters the absorber [4].

The absorber is the element that captures solar radiation and converts it into heat. To be able to do this effectively, it must be coated with a black paint or selective surface to increase the absorption coefficient to around 90%. Black paints are rapidly degraded at high temperatures and have an emissivity similar to the absorptivity for the long-wavelength range, which leads to considerable radiative losses. In contrast, selective surfaces are electrochemical treated so they can have low emissivity for this wavelength range. Currently, the most commonly selective surfaces used are copper coated with titanium or chromium [4].

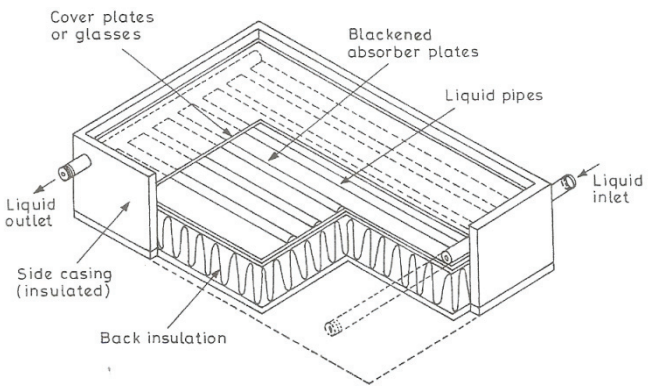

Figure 2. Schematic of a flat plate solar collector [5]

The thermal insulation serves to prevent heat losses, both at the bottom and sides of the collector. Given the high temperatures encountered in the operation of these equipments, insulation should not emit vapors and must withstand temperatures up to 150 °C without deteriorating [4].

The casing is the component which supports and protects each of the constituents of the solar collector, and acts as a link with the entire building on which it is housed through the anchoring elements previously installed. Among the most important characteristics of the casing, it must possess resistance to corrosion, variation of temperature and chemical instability [4].

2.1 MATHEMATICAL MODEL DESCRIPTION

The mathematical approach of the loss model used in this work is analogous to that proposed by Duffie and Beckman [6] and was based on the following assumptions:

- Performance is steady state.
- The headers cover a small area of the collector and can be neglected.
- The intake and discharge manifolds permit uniform flow distribution in the solar collector.
- The flow of heat through the transparent cover is one dimensional.
- The temperature drop through the transparent cover is negligible.
- The transparent cover is opaque to long-wavelength radiation.
- The flow of heat through the bottom and side insulation is one dimensional and can be treated independently.
- The sky can be considered as a black body for long-wavelength radiation at an equivalent sky temperature.
- Temperature gradient around the tubes can be neglected.
- Temperature gradients in the flow direction and between the tubes can be treated independently.
- Losses through different parts of the solar collector (top, bottom, sides) are related to the same ambient temperature.
- Dust and dirt on the transparent cover is negligible.
- Shading of the absorber plate is negligible.

The general energy balance for a flat plate solar collector is as follows:

$$\dot{q}_{in} = \dot{q}_L + \dot{q}_u \tag{1}$$

where:

$$\dot{q}_{in} = \tau\alpha I A_c \tag{2}$$

$$\dot{q}_L = U_L A_c \left(T_{pm} - T_{amb}\right) \tag{3}$$

The useful heat output of the solar collector, from Eqn (1), is as follows:

$$\dot{q}_u = A_c\left[\tau\alpha I - U_L\left(T_{pm} - T_{amb}\right)\right] \tag{4}$$

Energy efficiency is represented by Eqn (5):

$$\eta_{en} = \frac{\dot{q}_u}{IA_c} = \tau\alpha - \frac{U_L}{I}\left(T_{pm} - T_{amb}\right) \tag{5}$$

According to Duffie and Beckman [6] the transmissivity - absorptivity product should be treated as a property of the cover-absorber combination, which accounts for the interaction between the transparent cover and the absorber plate, and not simply as the multiplication of the transmissivity of the cover times the absorptivity of the absorber plate. To determine the value of this product, in Eqn (6) it is shown the approximation made by [6].

$$\left(\tau\alpha\right) \cong 1{,}01\tau\alpha \tag{6}$$

In practical applications, the fact that there is solar-energy absorption by the cover leads to an increase in its temperature, which causes a reduction in the heat loss flow from the absorber plate. Considering this, it is defined the effective transmissivity-absorptivity product $(\tau\alpha)_e$. The gain of $(\tau\alpha)_e$ regarding to that obtained by applying the assumptions previously stated, for a double transparent cover without a selective surface is approximately 2% [6]. Thus, when comparing experimental data with the theoretical results, Eqn (5) has to be modified as shown in Eqn (7).

$$\eta_{en} = \left(\tau\alpha\right)_e - \frac{U_L}{I}\left(T_{pm} - T_{amb}\right) \tag{7}$$

The fact that there are different types of constructive forms of absorbers is expressed, mathematically, by the called efficiency factor (F'). It is defined as the ratio of the useful energy provided by a collector, and the energy that it could supply if the absorber were at the mean fluid temperature, see Eqn (8) [7],

$$F' = \frac{\dot{q}_u}{\dot{q}_u\,|_{T_{pm}=T_{fm}}} \tag{8}$$

therefore the energetic efficiency is given as:

$$\eta_{en} = F'\left[\left(\tau\alpha\right)_e - \frac{U_L}{I}\left(T_{fm} - T_{amb}\right)\right] \tag{9}$$

Based on an energy balance alongside the fluid path with an infinitesimal length of tubing, and considering that the efficiency factor (F') and the overall heat transfer loss coefficient (U_L) are independent of position; the outlet temperature can be obtained from Eqn (10) [6].

$$\frac{T_{fo} - T_{amb} - S/U_L}{T_{fi} - T_{amb} - S/U_L} = exp\left(\frac{-U_L A_c F'}{\dot{m} C_p}\right) \tag{10}$$

where:

$$S = \left(\tau\alpha\right)_e I \tag{11}$$

Using the definition of the heat removal factor (F_R), the energy efficiency equation results as a function of the fluid inlet temperature, Eqn (12).

$$\eta_{en} = F_R\left[\left(\tau\alpha\right)_e - \frac{U_L}{I}\left(T_{fi} - T_{amb}\right)\right] \tag{12}$$

where:

$$F_R = \frac{\dot{m} C_p}{A_c U_L}\left[1 - exp\left(\frac{-U_L A_c F'}{\dot{m} C_p}\right)\right] \tag{13}$$

The mean fluid temperature is defined as follows, Eqn (14). According to Duffie and

Beckman [6] it is a common mistake to represent it as the average between the inlet and outlet temperatures.

$$T_{fm} = T_{fi} + \frac{qu \diagup A_c}{F_R U_L}\left(1 - F''\right) \tag{14}$$

where:

$$F'' = \frac{F_R}{F'} \tag{15}$$

The absorber mean temperature is defined as follows, see Eqn (16) [6]:

$$T_{pm} = T_{fi} + \frac{\dot{q}_u \diagup A_c}{F_R U_L}\left(1 - F_R\right) \tag{16}$$

Exergetic efficiency for a solar collection system which neglects the effect of pressure drop is defined as follows, Eqn (17) according [8].

$$\eta_{ex} = \frac{\dot{m}C_p\left(T_{fo} - T_{fi} - T_{amb}\ln\left(\frac{T_{fo}}{T_{fi}}\right)\right)}{IA_a\left(1 - \frac{T_{amb}}{T_{sun}}\right)} \tag{17}$$

The definition of exegetic efficiency has generated controversy because of the different expressions reported over the years to represent the exergy of solar energy. The first relation, see Eqn (18), was raised by Petela [9], and it is based on how a piston system that has a black body radiation trapped in an initial state (V_1, T_1) gives his work as it reaches a maximum dead state (V_2, T_2), where $T_2 = T_{amb}$ by a reversible and adiabatic expansion. Bejan [10] reaches the same expression of Eqn (18) by two independent ways.

$$\eta_p = \frac{W_{1-2}}{U_1} = \left[1 - \frac{4}{3}\frac{T_2}{T_1} + \frac{1}{3}\left(\frac{T_2}{T_1}\right)^4\right] \tag{18}$$

The other most significant efficiency ratios that have been proposed instead of Eqn (18) are those of Spanner and Jeter [10]. According to [10], the equations of Petela, Spanner and Jeter seem to compete with each other, when, in fact, are complementary because each equation represents parts of the domain of the studied phenomenon. This was represented by Bejan [10] as a three-stage reversible process: filling based on a T_1 source system to reach the state 1, expansion (state 1 - 2) and discharge to a sink T_2 (state 3).

2.2 SOLAR COLLECTOR PREDICTIVE ALGORITHM

The developed algorithm for determining operating parameters of the solar collector, such as the energy and exergy efficiency is shown in Figure 3 and consists of a system of iterative calculations with two nested loops. Unlike the algorithm of Farahat *et al.* [8], this one allows the variability of wind velocity, relative humidity and incidence angle at any time of the day, improving the accuracy of the prediction.

The program starts when the user enters the input variables, which were classified into three groups:

- Concerning the location and date of use: latitude and longitude of the installation, tilt and azimuth angles of the collector; day, month, standard time and time zone for its determination.
- Related to the equipment: collector physical dimensions, properties of the materials used, $(ta)_{e,n}$, and incident angle modifier (K_{ta}).
- Relative to the operation of the collector: mass flow rate; ambient, sky and working fluid input temperatures; wind velocity and irradiance.

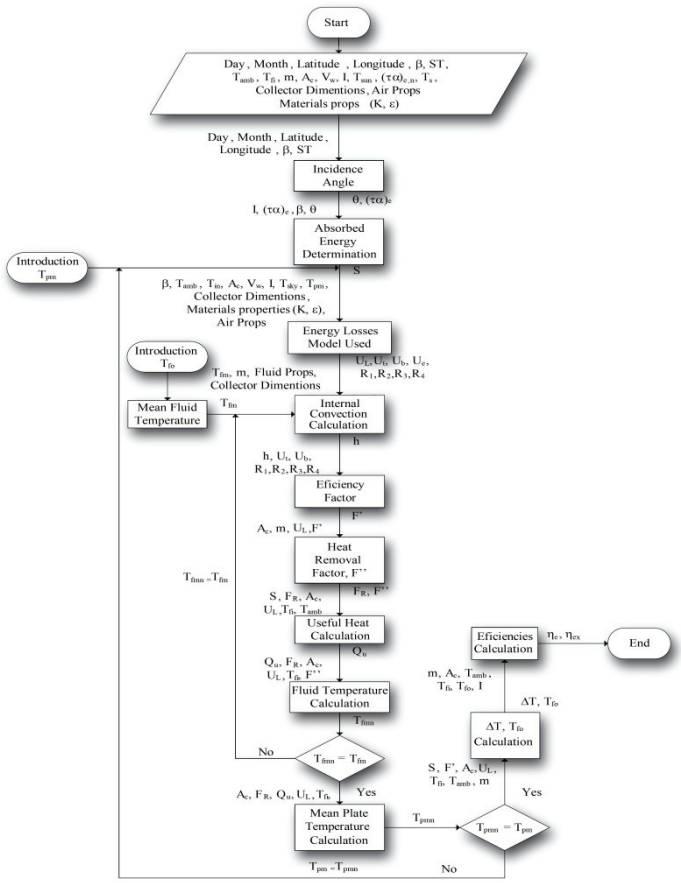

Figure 3. Solar collector performance prediction algorithm

Upon completion of this step, the algorithm proceeds to do its preliminary calculations, which are the determination of the incidence angle for the time of the study and with it, the input power (S) of the absorber. This parameter is entered in the first iterative loop for the establishment of the average temperature of the absorber plate. Here, it begins with the calculation seed referred to the fluid input temperature, the data concerning the operation and the type of collector used, and enters into the calculation of the heat transfer loss model, in which an iterative calculation is done to determine the overall loss coefficient (U_L).

After finishing the heat-transfer model block, the algorithm enters into the second loop that corresponds to the establishment of the mean fluid temperature (T_{fm}). Here, several important parameters of the equipment are calculated, such as: efficiency factor (F'), heat removal factor (F_R) and flow factor (F''), to close the loop with the calculation of the new T_{fm}, using Eqn (14).

When the mean fluid temperature obtained complies with the tolerance set by the user, the algorithm passes to the calculation of the new average temperature of the plate, using Eqn (16), which is then compared with the assumed value. Upon completion, the output temperature (T_{fo}) is determined. Finally, the algorithm calculates the energy and exergy efficiencies, ending the program.

2.3 ALGORITHM PERFORMANCE TESTS

Before beginning the performance tests, it was ensured that the results were independent of the seeds and tolerances used. When completed, it was performed a sensitivity analysis to test the logic of the results reported by the algorithm. The first one consisted in the determination of the overall heat loss coefficient and the energy and exergy efficiency, under a Gaussian distribution of the solar irradiance over time. The irradiance trend was based on a data correspondent to the date 09/26/2009 available from the Simon Bolivar University weather station. The parameters considered constant were the following: mass flow rate of 0.0034 kg/s, fluid inlet and ambient temperature of 25 °C, relative humidity of 60%, wind velocity of 2.33 m/s west-east direction, see Figure 4.

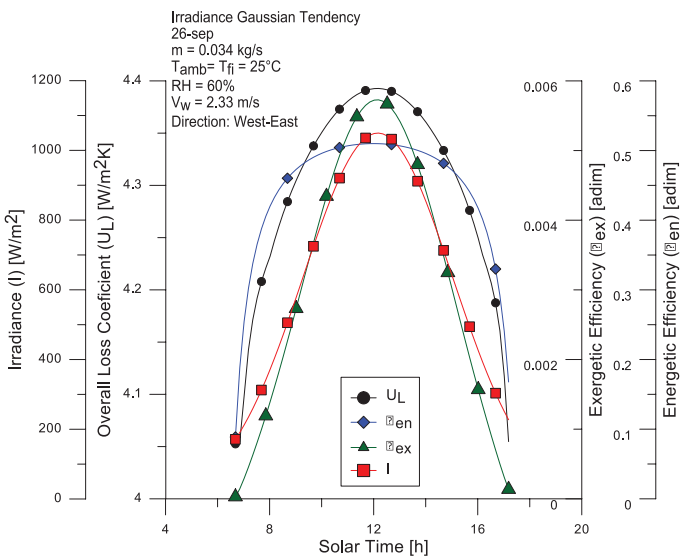

Figure 4. Sensitivity analysis based on a Gaussian trend irradiance variability

In Figure 4, it can be seen the maxima of the variables are close to solar noon, which is consistent with the behavior reported by González-Acuña [11]. The maximum of the overall heat loss coefficient was approximately 4.4 W/m^{2}K, a value similar to the one reported by [2] and [8]. In the meantime, the values of energy and exergy efficiencies were about 50% and 5.5%, respectively. These values demonstrate that the developed algorithm exports logic results and is also coherent with commercially available equipment on the market.

Figure 5 shows the behavior of the global exergetic efficiency, the mass flow required to achieve it, and the gain temperature ΔT that result under this operation condition, depending on the fluid inlet temperature. It can be appreciated that the efficiency has a downwardly concave behavior, which means that the solar collector has an absolute maximum exergetic efficiency of 6.5% when the inlet temperature is around 335 K, with a mass flow close to 0.0040 kg/s (0.24 LPM).

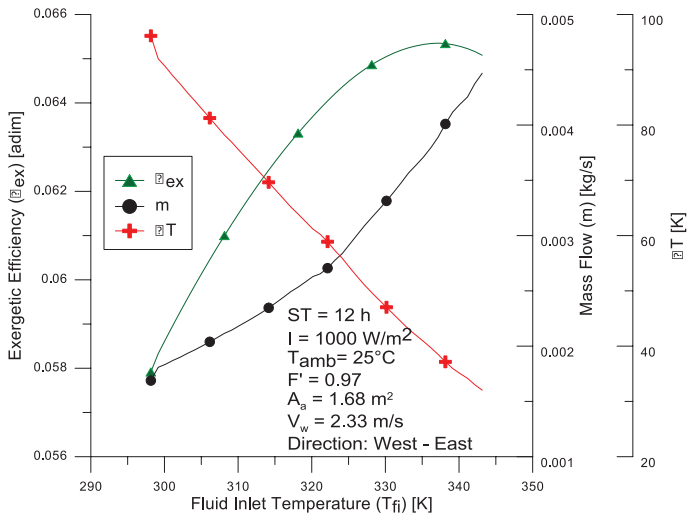

Figure 5. Sensitivity analysis of global exergetic efficiency based on fluid inlet temperature

In regard to the mass flow behavior, it can be observed a proportional with the inlet temperature. Physically, it means as the inlet temperature augments, the mass flow must be increased to maintain the overall efficiency condition, which entails a decreasing DT as this happens. Such behavior is expected by the form of the temperature gain expression, see Eqn (10).

It is noteworthy that the calculation algorithm and heat loss model used, which consisted on the thermal resistance scheme described by Duffie and Beckman [6], were validated against experimental data. The solar collector tested, in real weather conditions, was a sandwich type solar collector, and the testing rig was designed and constructed based on the ANSI/ASHRAE 93-2003 standard [3] requirements. The validation process is not addressed in the present work [11].

3. SOLAR COLLECTOR EXERGY OPTIMIZATION

The operation criteria establishment for maximum exergetic gain of the working fluid across the solar collector built in the desalination unit was performed using real meteorological data, collected by the weather station at Simon Bolivar University in a calendar year (September 26th, 2009-2010) [12]. Of all the available parameters, those selected as priorities for this phase, were ambient temperature and irradiance. It is noteworthy that the solar resource on a horizontal surface was extrapolated to a tilt and azimuth angle of 10.5° and 0°, respectively, corresponding to the orientation of the collector tested.

Two scenarios were considered, one in which the ambient and the fluid inlet temperature were the same, see Figure 6, and the other where the inlet temperature was fixed at 54°C (327 K), the design point for the desalination plant, see Figure 7. For this, a wind velocity of 2.33 m/s with a west-east direction and a relative humidity of 60% were considered constant.

The optimum operating mass flow rate was determined by the developed algorithm, focusing it on the search of the absolute maximum exergy efficiency for those environmental conditions registered. This efficiency point meant, for a defined aperture area of 1.68 m^2, a specific mass flow rate as shown in Eqn (17). Finally, the different variables were plotted considering only daylight hours, similar with reported by Badescu [13].

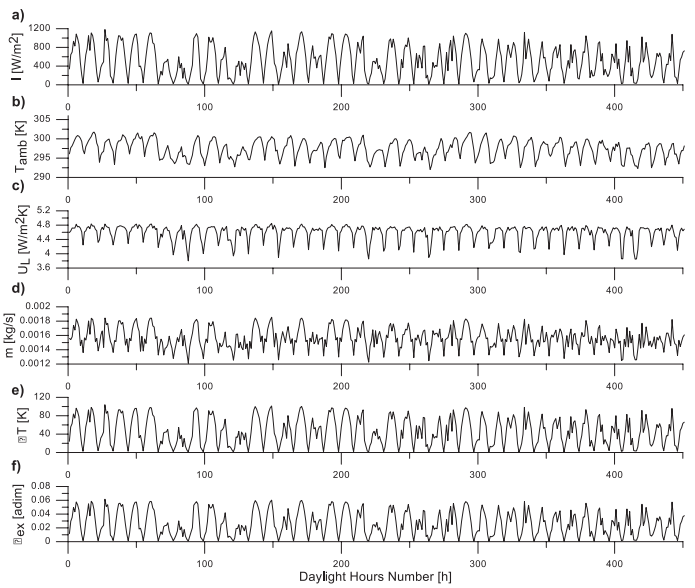

Figure 6. Operation to maximize exergetic efficiency for the scenario where $T_{fi} = T_{amb}$

In Figure 6, it can be seeing the irradiance as well as the rest of the variables involved in the analysis, presented a periodic behavior with a maximum value, which occurred at solar noon. The ambient temperature, for the same time period, was above 300 K on most of the days reported. The combination of such climate conditions, led to a maximum U_L coefficient of 4.8 W/m^2K, and an optimal mass flow of 0.0018 kg/s. This variable was entirely alternate around 0.0016 kg/s, without presenting any significant pattern.

The alternative behavior of the optimal mass flow shown in Figure 6 differs from that reported by [13], where it was observed for the condition T_{fi} = 300 K an almost constant mass flow rate per unit of area of 0.0010 kgm^{-2}/s. Multiplying this number time the aperture area of the collector studied in the present work (1.68 m^2), results in the value of 0.0017 kg/s, very similar to the flow discussed in the preceding paragraph, which places both investigations in this regard under the same order of magnitude.

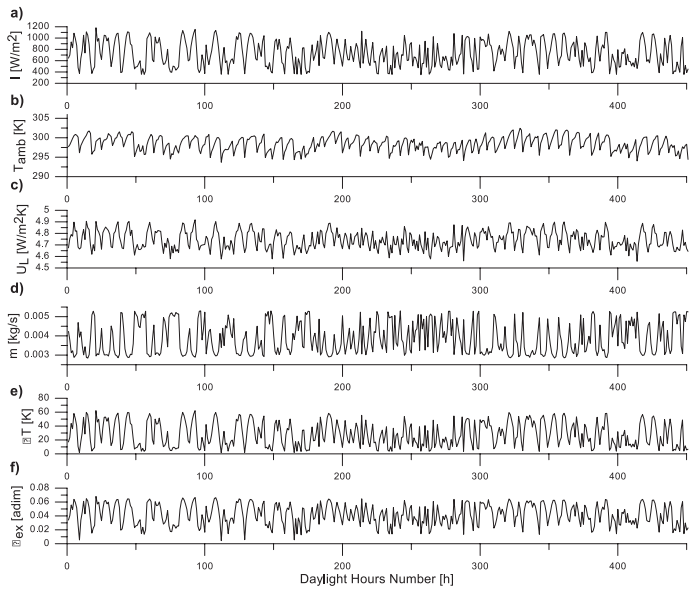

Figure 7. Operation to maximize exergetic efficiency for the scenario where T_{fi} = 327 K

Considering the temperature gain ΔT of the working fluid within the optimum flow rate operation, it can be seen in Figure 6 that it exceeded 80 K at solar noon on most of the days reported. This implies that the outlet temperature of the collector would be above 380 K. For collectors used in domestic hot-water applications, which meet the condition referred to this scenario, the discharge temperature is very high and can compromise the thermal resistance of the components, especially the isolation of those built on a low budget. It must be noted that the empirical correlations employed in the simulation of this system are referred to flow without the presence of phase change. The operation pressure to meet this premise should be above 300 kPa (3 bar).

In assessing the irradiance in Figure 7, it can be seen that almost no points are below 400 W/m^2. It was found, for this scenario, that an irradiance below 350 W/m^2 entailed a negative ΔT of the working fluid. This means the equipment is functioning as a heat sink, implying a negative exergy efficiency, which was not representative for the purposes of the analysis, although it served to define the stopping criteria of the desalination plant. It is noteworthy to observe the elimination of the values below the limit of irradiance in Figure 7.

In regard to the U_L coefficient, it was found an increase of the mean and maximum value, as would be expected by increasing the inlet temperature, as shown in Figure 7. Likewise,

the optimum mass flow rate maintained its alternative character and increased its value consistently with that reported in Figure 5 to a maximum 0.005 kg/s at solar noon. In this manner, it was found a disagreement with the statements made by Badescu [13], not only in the behavior of the variable, since the quantity considered as mean presented a wide difference. In this work, the optimum mass flow rate for inlet temperatures of 300 and 320 K showed the same average value for both scenarios [13].

The maximum ΔT obtained by the working fluid in Figure 7 was 60 K, which is a decrease with the observed in Figure 6. Despite this, such a reduction still means a collector discharge temperature above 373 K.

The maximum pressure of the sandwich type solar collector characterized was three meters of liquid column [11]. This limitation forced to limit the ΔT to 35 K, which meant a discharge temperature of 362 K, a value that can be considered as valid for the assumptions made. To achieve this, it was necessary not only increased the amount of mass flow; also its erratic nature has to be considered, to guarantee not to reach the boiling point at the atmospheric pressure in presence of solar radiation intensification.

As the exergetic efficiency is concerned; it reached a maximum value of 6.4%, about 0.4% less than recorded in Figure 7, resulting in a 6% loss in power quality by this limitation. This results in an annualized decrease of 1%, which is negligible.

Considering that the desalination system was designed to be placed in remote areas with little access, it was established a fixed mass flow operation rate of 0.006 kg/s (0.36 LPM) which allowed to get as close as possible to the maximum exergetic efficiency in Figure 7 without getting to the boiling point. This meant a maximum efficiency of 6.3%, with a decrease in annualized efficiency, compared to the behavior shown in Figure 7, of 4%.

4. CONCLUSIONS

- It was developed a calculation algorithm that allowed improving the accuracy on the solar collector performance prediction, considering the variability of wind velocity, relative humidity and incidence angle at any time of the day.
- The results obtained from the sensitivity analysis of the performance algorithm showed a logic behavior of the variables tested, and coherence with commercially available equipment on the market.
- It exists a global maximum exergetic efficiency of 6.5% when the inlet temperature is around 335 K, for the environmental conditions in which the test was performed.
- The operation criterion to maximize exergy efficiency when the collector is operating in domestic hot-water applications did not show the behavior reported by Badescu, even though mean values of the required mass flow rates were similar in this purpose.
- The working fluid pressure required to avoid phase change in the point of maximum exergetic efficiency, was found to be above 300 kPa (3 bar).
- To maximize the gain of exergy of the sandwich type flat plate solar collector built for a MEH desalination plant, it should operate under a fixed mass flow criterion of 0.006 kg/s (0.36 LPM).
- The operation of the solar collector should stop when the irradiance decreases below 350 W/m^2.

REFERENCES

González, R., Pieretti, P. y Díaz, H., Design algorithm of a multi-effect humidification-dehumidification solar distillation system, in: Beale, S. ed(s) *Proceedings of the ASME 2009 International Mechanical Engineering Congress & Exposition IMECE2009,* ASME, Lake Buena Vista, Florida, USA, 2009, pp. 111-115.

Luminosu, I. and Fara, L., Determination of the optimal operation mode of a flat solar collector by exergetic analysis and numerical simulation, *Energy*, 2005, Vol.30, pp.731-747.

ANSI/ASHRAE 93-2003 Standard, *Methods of testing to determine the thermal performance of solar collectors*, American Society of Heating, Refrigerating and Air-Conditioning Engineers, 2003.

Bayo, M., *Diseño e Instalación de Arreglos Fotovoltaicos y Térmicos*, Instituto de Energía (INDENE), Caracas, 2007, pp.10 – 45.

Tiwari, G.N., *Solar energy fundamentals, design, modeling and applications,* Alpha Science, 2004, pp.94-116.

Duffie, J.A. and Beckman, W.A. *Solar engineering of thermal processes*, Third Edition, Wiley, 2006, pp.289-304.

Peuser, F., Heinz Remmers, K., and Schnauss, M., *Sistemas solares térmicos, diseño e instalación*, CENSOLAR, 2005, pp.129-157.

Farahat, S., Sarhaddi, F. and Ajam, H., Exergetic optimization of flat plate solar collectors, *Renewable Energy*, 2009, Vol.34, pp.1169-1174.

Petela, R., Exergy of heat radiation, *ASME Journal of Heat Transfer*, 1964, Vol.86, pp.187-192.

Bejan A., *Advanced Engineering Thermodynamics*, Third edition, Wiley, 2006, pp.102-448.

González-Acuña, R., *Caracterización y Optimización Exergética de un Colector de Placa Plana para Desalinización Solar*, Master in Science, Universidad Simón Bolívar, Caracas, 2012.

Simon Bolivar University Weather Station Data. Retrieved April 18th, 2011 from: http://cbm.usb.ve/clima/informacion.html#datos.

Badescu, V., Optimal control of flow in solar collectors for maximum exergy extraction, *International Journal of Heat and Mass Transfer*, 2007, Vol.50, pp.4311-4322.